Available online at www.sciencedirect.com
SCIENCE DIRECT®
Biochemical Pharmacology 66 (2003) 191–202
Biochemical Pharmacology
www.elsevier.com/locate/biochempharm

Inhibition of cholinesterases with cationic phosphonyl oximes highlights distinctive properties of the charged pyridine groups of quaternary oxime reactivators☆

Yacov Ashani[a,1], Apurba K. Bhattacharjee[b], Haim Leader[a,1], Ashima Saxena[a,*], Bhupendra P. Doctor[a]

[a]*Division of Biochemistry, Walter Reed Army Institute of Research, 503 Robert Grant Road, Silver Spring, MD 20910-7500, USA*
[b]*Division of Experimental Therapeutics, Walter Reed Army Institute of Research, 503 Robert Grant Road, Silver Spring, MD 20910-7500, USA*

Received 12 July 2002; accepted 11 November 2002

Abstract

Oxime-induced reactivation of phosphonylated cholinesterases (ChEs) produces charged phosphonyl pyridine oxime intermediates (POXs) that are most potent organophosphate (OP) inhibitors of ChEs. To understand the role of cationic pyridine oxime leaving groups in the enhanced anti-ChE activity of POXs, the bimolecular rate constants for the inhibition (k_i) of acetylcholinesterases (AChE) and butyrylcholinesterases (BChE), and the rate of decomposition (k_d) of authentic *O*-alkyl methylphosphonyl pyridine oximes (AlkMeP-POXs) and *N*,*N*-dimethylamidophosphoryl pyridine oximes (EDMP-POXs), were studied. Stability ranking order in aqueous solutions correlated well with the electronic features and optimized geometries that were obtained by *ab initio* calculations at 6-31G** basis set level. AlkMeP-POXs of the 2-pyridine oxime series were found to be 4- to 8-fold more stable ($t_{1/2}$ = 0.7 to 1.5 min) than the homologous *O*,*O*-diethylphosphoryl (DEP) oxime. Results suggest that re-inhibition of enzyme activity by POX is less likely during the reactivation of DEP–ChEs (obtained by use of DEP-containing pesticides) by certain oximes, compared to nerve agent-inhibited ChEs. The greatest inhibition was observed for the *O*-cyclohexyl methylphosphonyl-2PAM derivative (4.0×10^9 M^{-1} min^{-1}; mouse AChE) and is 10-fold higher than the k_i of cyclosarin. Increasing the size of the *O*-alkyl substituent of AlkMeP-POXs had only a small to moderate effect on the k_i of ChEs, signifying a major role for the cationic pyridine oxime leaving group in the inhibition reaction. The shape of plots of log k_i vs. pK_a of the leaving groups for AlkMeP-PAMs and DEP-PAMs, could be used as a diagnostic tool to highlight and rationalize the unique properties of the cationic moiety of pyridine oxime reactivators.

Keywords: Cholinesterases; Inhibition; Decomposition; Organophosphates; Phosphonyl oximes; *Ab initio*

☆ A preliminary communication was presented at The US Army Medical Defense Bioscience Review 2000, 4–9 June, Hunt Valley Inn, MD.

* Corresponding author. Tel.: +1-301-319-9406; fax: +1-301-319-9150.
E-mail address: ashima.saxena@na.amedd.army.mil (A. Saxena).

[1] Recipients of the National Research Council fellowship; on sabbatical leave from Israel Institute for Biological Research, P.O. Box 19, Ness Ziona, Israel.

Abbreviations: ChE, cholinesterases; AChE, acetylcholinesterase; BChE, butyrylcholinesterase; rMoAChE, recombinant mouse AChE; FBS AChE, fetal bovine serum AChE; HuBChE, human BChE; EqBChE, equine BChE; OP, organophosphates; 2-PAM, 1-methyl-2-pyridinium carboxaldehyde oxime; POX, phosphonyl, phosphoryl, or dimethylamidophosphoryl pyridine oximes; AlkMeP-POXs, *O*-alkyl methylphosphonyl pyridine oximes; DEP, *O*,*O*-diethylphosphate; DEPQ, 7-(*O*,*O*-diethylphosphinyloxy)-1-methylquinolinium methyl sulfate; MEPQ, 7-(*O*-ethyl methylphosphinyloxy)-1-methylquinolinium iodide; DEP-POX, *O*,*O*-diethylphosphoryl pyridine oximes; DEP-TMP, 3-(*O*,*O*-diethylphosphinyloxy)-*m*-(*N*,*N*,*N*-trimethylammonio) phenyl iodide; DEP-MHP, 3-(*O*,*O*-diethylphosphinyloxy)-1-methyl pyridinium iodide; EDMP-POXs, *O*-ethyl *N*,*N*-dimethylamidophosphoryl oximes; IMP-thiocholine, *O*-isopropyl *S*-(*N*,*N*,*N*-trimethylammonio ethyl)methylphosphonothiolate; CNPY, cyanopyridinium cations; MEP, molecular electrostatic potentials.

0006-2952/03/$ – see front matter © 2003 Elsevier Science Inc. All rights reserved.
doi:10.1016/S0006-2952(03)00204-1

1. Introduction

Phosphonylated oximes (POXs, Fig. 1) are intermediates formed during oxime-induced reactivation of OP-inhibited ChEs (Fig. 2a). The POXs listed in Table 1 are expected to accumulate during the reactivation of AChEs inhibited with the G- and V-type nerve-agents and with diethylphosphate-based pesticides (Fig. 1), by a variety of quaternary pyridine oximes. The re-inhibition of enzymatic activity by POX slows down the regeneration of AChE activity and complicates the interpretation of results from kinetic studies both *in vitro* and *in vivo*. The antidotal potency of an oxime reactivator against OP toxicity depends mostly on the apparent rate by which it displaces the OP residue from its covalent attachment to AChE. For this reason, the rapid decomposition of POX, accumulated during oxime treatment of OP poisoning, is of considerable importance for the therapeutic management of nerve agent and pesticide poisoning.

Inhibition of AChE (EC 3.1.1.7) and BChE (EC 3.1.1.8) by OPs yield covalent conjugates with the active-site serine located at the bottom of a deep narrow gorge [1,2]. In contrast to cationic aliphatic OPs, the potential for charge dispersion on a planar cationic aromatic system such as POX may provide a large unsymmetrically charged surface capable of interactions with negative electrostatic potential sites at the entrance and along the catalytic gorge.

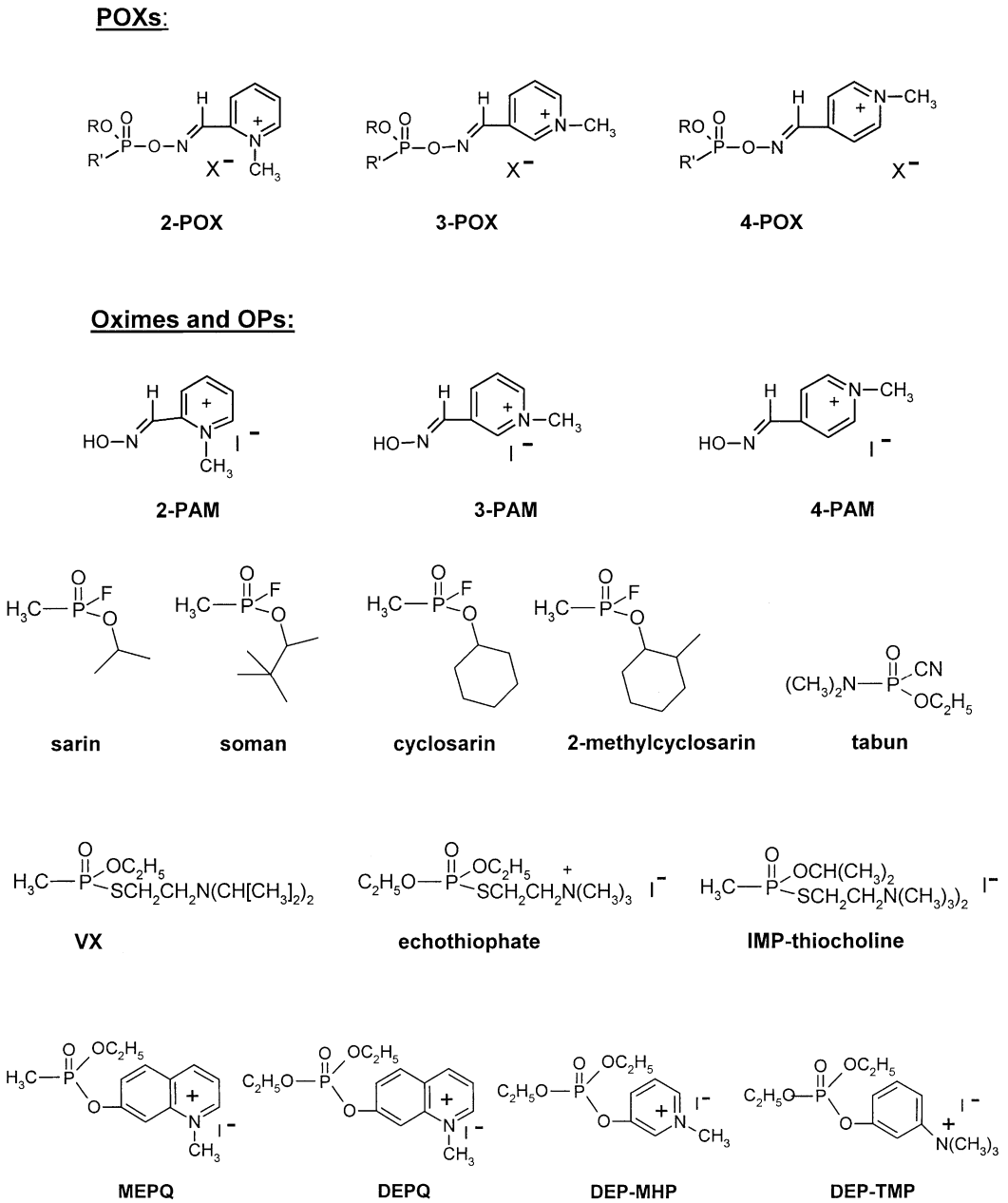

Fig. 1. Structures of organophosphate inhibitors and pyridine oxime reactivators. The *syn* isomers of POXs and PAMs are shown. When $R' = CH_3$ and R = Et, iPr, pinacolyl, cyclohexyl, and 2-methylcyclohexyl, the POXs represent the parent OP inhibitors VX, sarin, soman, cyclosarin, and 2-methylcyclosarin, respectively. When $R' = (CH_3)_2N$ and R = OEt, the parent inhibitor is tabun.

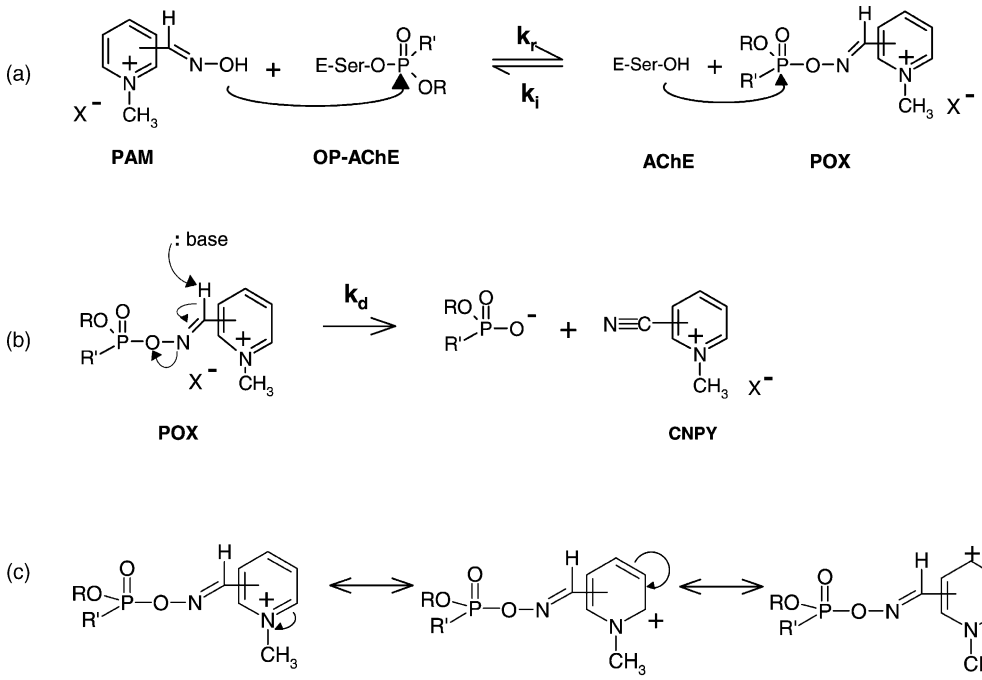

Fig. 2. Reaction pathways associated with POXs. (a) Reactivation and re-inhibition; (b) Decomposition in accordance with the β-elimination reaction; (c) Resonance stabilization of the dispersed positive charge on the pyridine ring.

Table 1
Rate constants for the decomposition of POXs ($t_{1,2}$) and the inhibition of ChEs by POXs (k_i)[a]

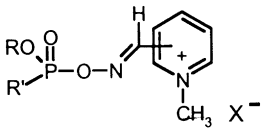

POX	R	R′	$t_{1/2}$[b] (min)	10^{-6} k_i[c] (M^{-1} min^{-1})			
				rMoAChE	FBS AChE	HuBChE	EqBChE
EMP-2PAM	C_2H_5	CH_3	0.70	1940	3590	1630	280
IMP-2PAM	$CH(CH_3)_2$	CH_3	1.05	1420	2170	632	42
PMP-2PAM	$CH(CH_3)C(CH_3)_3$	CH_3	1.50	1570	1070	236	139
CMP-2PAM	Cyclohexyl	CH_3	1.30	4020	2800	672	211
MCMP-2PAM	2-Methylcyclohexyl	CH_3	0.79	3400	2740	840	244
EDMP-2PAM	C_2H_5	$(CH_3)_2N$	1.10	11	14	3.7	3.0
DEP-2PAM[d]	C_2H_5	C_2H_5	0.18	210	140	2030	140
EMP-3 PAM	C_2H_5	CH_3	588	2.7	1.9	34	1.2
CMP-3 PAM	Cyclohexyl	CH_3	>600	195	89	401	44
DEP-3 PAM	C_2H_5	C_2H_5	139	0.16	0.084	66	0.92
EMP-4PAM	C_2H_5	CH_3	62	382	188	296	69
IMP-4PAM	$CH(CH_3)_2$	CH_3	75	110	60	73	12
PMP-4PAM	$CH(CH_3)C(CH_3)_3$	CH_3	112	237	159	363	29
CMP-4PAM	Cyclohexyl	CH_3	84	1800	1580	1860	265
MCMP-4PAM	2-Methylcyclohexyl	CH_3	100	596	251	823	137
EDMP-4PAM	C_2H_5	$(CH_3)_2N$	63	2.5	1.4	2.2	0.44
DEP-4PAM[d]	C_2H_5	C_2H_5	16	6.0	1.0	710	40
MEPQ				1980		1380	290
DEPQ				660		4420	532
Echothiophate				7.0		7.7	2.1

[a] For structural details see Fig. 1. EMP-, IMP-, PMP-, CMP-, MCMP-, EDMP- and DEP-POXs are expected during reactivation of ChEs inhibited with VX, sarin, soman, cyclosarin, 2-methylcyclosarin, tabun, and paraoxon, respectively.
[b] Mean of 3–6 determinations ±SD < 20%.
[c] Mean of 4–9 determinations, ±SD < 20%, except for DEP-4PAM vs. EqBChE (±SD = 35%).
[d] From [9].

For example, the bimolecular rate constants (k_i) for the inhibition of AChEs from various sources by the cationic aromatic ligands DEPQ and MEPQ (Fig. 1) were found to be $1-5 \times 10^8$ M^{-1} min^{-1} [3–5], while those of homologous cationic aliphatic OPs such as echothiophate or one of its methylphosphonate analogs, IMP-thiocholine (Fig. 1), were reported at 0.06 to 0.16×10^8 M^{-1} min^{-1} [6–8]. The remarkably high k_i values of DEPQ and MEPQ relative to those of echothiophate and IMP-thiocholine may be explained by the >100-fold increase in acidity of the 1-methyl 7-hydroxyquinolinium leaving group ($pK_a = 5.7$; [4]) compared to that of thiocholine ($pK_a \sim 7.7$; [9]). However, results from recent experiments generated k_i values of $91-130 \times 10^8$ M^{-1} min^{-1} for certain bis-quaternary aromatic OPs of the phosphonyl oxime family with leaving groups exhibiting pK_a values near 8.2 [3]. The three phosphonylated oxime series depicted in Fig. 1 and listed in Table 1 are structurally related to the most potent OP inhibitors of ChE, namely, bis-quaternary phosphonyl oximes [3]. Hence, they offer suitable candidates for the systematic evaluation of the effect of charge delocalization and molecular geometry on the rate of ChE inhibition, and on the stability of POXs in aqueous solutions.

Previous studies reported on the *in situ* characterization of AlkMeP-POX [3,10–14] and DEP-POX [11,12]. Only recently have authentic DEP-POXs been synthesized and characterized as anti-ChEs [15]. We report here on the experimental and theoretical studies of 12 newly synthesized AlkMeP-POXs and two EDMP-POXs. It is suggested that the enhanced anti-ChE activity of POXs and their stability ranking order arise from the unique properties of the positive electrostatic potential of the charged aromatic leaving group. Results also highlight the contribution of an *O*-cyclohexyl substituent to the increased anti-ChE potency of OPs.

2. Materials and methods

2.1. Materials

AlkMeP-POXs and EDMP-POXs were prepared using procedures described earlier for the synthesis of DEP-POXs [15]. Briefly, tertiary POXs of 2-, 3- or 4-pyridine carboxaldehyde oxime were obtained by reacting the relatively non-toxic *O*-alkyl methylphosphonochloridates or *O*-ethyl *N*,*N*-dimethylamidophosphorochloridate with the corresponding pyridine carboxaldehyde oxime (Aldrich Chemical Co). The tertiary POXs were purified by column chromatography and converted to quaternary compounds in the presence of excess methyl iodide or dimethyl sulfate in CH_3CN at room temperature. DEP-3PAM was prepared using the procedure previously described for DEP-4PAM [15]. The DEP esters of the cations *m*-(*N*,*N*,*N*-trimethylammonio) phenol iodide (DEP-TMP) and 1-methyl 3-hydroxy pyridinium iodide (DEP-MHP) were prepared by reacting the tertiary amines with *O*,*O*-diethylphosphoryl chloride followed by quaternization with methyl iodide. The completion of all reactions and the purity of the new compounds were established by TLC and ^{31}P, ^{1}H, and ^{13}C NMR spectroscopy. MEPQ and DEPQ were prepared as described earlier ([5] and [16], respectively), and echothiophate was obtained from Ayerst Laboratories.

Purified rMoAChE was provided by Professor P. Taylor and Dr. Z. Radić. FBS AChE, HuBChE, and EqBChE were purified by procainamide-Sepharose 4B gel-affinity chromatography [17,18].

2.2. Enzyme assays

The activities of ChEs were determined by the method of Ellman *et al.* [19] using 1 mM acetylthiocholine iodide and butyrylthiocholine iodide as substrates for AChE and BChE, respectively. Assays were carried out in 50 mM phosphate buffer, pH 8.0, at 25°.

2.3. Determination of k_d and k_i

Fresh aqueous stock solutions of POXs (approximately 10 μM) adjusted to pH 4.5 by adding a few drops of 0.1 M acetate buffer, were kept in an ice-water bath. The concentrations of stock solutions were confirmed further by titration of a known concentration of HuBChE pre-determined by use of DEPQ [16]. The decomposition rate constants (k_d) for various POXs, and the rate constants for the inhibition of AChEs and BChEs by POXs (k_i) were determined essentially as described [15], using 10 mM HEPES buffer, pH 7.8, at 29°.

2.3.1. Decomposition of POXs

The decomposition of 2- and 4-POXs were determined by monitoring decreases in absorbance at 278 and 254 nm, respectively. The decomposition of the 3-POX series was based on a decrease in absorbance at 273 and an increase at 267 nm. Rate constants were calculated using the following equation:

$$OD_t - OD_\infty = (OD_0 - OD_\infty)\, e^{-k_d t} \quad (1)$$

where, OD_0 and OD_t are the absorbances at time zero and at time t, respectively. OD_∞ is the value assigned when no changes in absorbance were observed. In all cases, the decomposition products were identified by UV spectra. Results were compared to standard solutions of authentic 2-, 3-, and 4-CNPY prepared as previously described [15]. In several cases, these k_d values were validated by determining the rates at which the POXs lost their anti-ChE activity.

2.3.2. Inhibition of ChEs

At $t = 0$, an aliquot of a stock solution of POX was diluted into 10 mM HEPES buffer, pH 7.8, containing

ChE and 0.1% BSA, and pre-incubated at 29°. The final concentrations of the inhibitors were sufficiently high to establish pseudo-first-order reaction conditions. For 3- and 4-POXs, curve-fitting of the data points was carried out by nonlinear regression analysis using the mono-exponential decay equation:

$$E_t = E_0\, e^{-k_{obs}t} \quad (2)$$

where, E_t and E_0 are enzyme activities at time t and zero, respectively. k_i was calculated from the slope of the straight line obtained by the plot of k_{obs} vs. [POX]. Due to the rapid decomposition of all 2-POXs, k_i was determined as previously described for DEP-2PAM [15]. Briefly, as time increases, the ratio of the residual enzyme to its initial activity approaches a limiting value as shown in Eq. (3):

$$\ln\left(\frac{E_\infty}{E_0}\right) = -[\text{2-POX}]_0\left(\frac{k_i}{k_d}\right) \quad (3)$$

where E_∞ is the enzyme activity that does not change over 15 min, and E_0 is the activity at time zero. $[\text{2-POX}]_0$ is the initial concentration of the tested POX. k_i was calculated from Eq. (3) using the value of k_d obtained as described above.

2.4. Hydrolysis of DEPQ

The bimolecular rate constant for the hydroxide-induced hydrolysis of DEPQ was determined by monitoring the increase in absorbance of the leaving group 1-methyl 7-hydroxyquinolinium at 406 nm, in the presence of 0.01 to 0.1 NaOH.

2.5. Quantum chemical calculations

The geometry and electronic features of the POXs were calculated using quantum chemical AM1 and *ab initio* methods. Several low energy conformers with varying population densities were generated using the systematic search technique via AM1 method as implemented in SPARTAN version 5.1.2 (Wavefunction, Inc.). The geometry of the minimum energy and most abundant conformer was considered for further optimization and calculation of electronic properties. Geometry optimization and energetics calculations were performed using the Gaussian 94 version (Revision A.1).

3. Results

3.1. Structures of POXs

All NMR signals were in agreement with the proposed structures and suggest that only one kind of geometrical isomer was isolated. On the basis of the published NMR chemical shifts and coupling constants of well-defined *syn* and *anti* pyridine aldoximes and their quaternary salts,[2] it is proposed that the OP moieties of POXs listed in Table 1, are *syn* to the carboxaldehyde hydrogen, P−O−N=C(H)−Cpyr. This assignment implies that the *syn* geometry of the starting materials (i.e. the tertiary oximes) was conserved. As was demonstrated previously with DEP-POXs [15], the anti-parallel orientation of the bulky OP and pyridine moieties seems to be the preferred geometry in all POXs and is consistent with the X-ray crystal structure of IMP-4PAM [20].

3.2. Decomposition of POXs

Based on spectral changes in aqueous solutions, and a comparison of the UV spectra of the decomposition products with authentic samples, the major decomposition products were identified as the corresponding CNPY cations (Fig. 2b). This observation is consistent with previous reports ([15], and references cited therein).

The $t_{1/2}$ values of AlkMeP-2PAMs and EDMP-2PAM were 0.7 to 1.5 min (Table 1), while those for the 4-POXs series were 57- to 126-fold higher, approaching a value of 112 min for PMP-4PAM. When the OP-oxime moiety was at the meta-position of the pyridine ring (3-POXs), a further increase in stability was observed ($t_{1/2} > 580$ min). A similar dependency on the position of the OP-oxime moiety was observed for the decomposition rates for DEP-POXs. However, DEP-POXs decomposed at rates that were 4- to 8-fold higher than those of AlkMeP-POX and EDMP-POXs. In the 2- and 4-POXs, the change from an ethyl (EMP-POXs) to a pinacolyl group (PMP-POXs) resulted in a ~2-fold increase in stability, which can be attributed to a combined effect of steric factors and an increased electron donation by the pinacolyl group.

3.3. Inhibition of ChEs

AlkMeP-POXs and EDMP-POXs are racemic mixtures of 2 or 4 enantiomers. Since replacement of thiocholine with the pyridine oxime function does not change the definition of absolute configuration, it is assumed that the enantiomers with the Sp assigned configuration [7] are also the active isomers of POXs. The enantioselectivity ratio Sp/Rp for AChEs could be appreciated only with the relatively stable 4-POX series. Based on the titration of pre-determined concentrations of rMoAChE, a significant enantioselectivity was displayed by all 4-POXs with the exception of EMP-4PAM, which showed a reduced enantioselectivity (not shown).[3] This observation is consistent with the behavior of homologous *O*-ethyl methylphosphonates with different leaving groups, such

[2] For literature citations see [15]. The *syn* configuration of the active geometrical form of 2-, 3- and 4-PAM are depicted in Fig. 1.

[3] A 1:2 molar ratio of AChE to racemic POX was required to inhibit 100% of enzyme activity; less than 2 mol were required to produce complete inhibition with EMP-4PAM.

as MEPQ and VX [5,21]. As rationalized before for *O*-alkyl methylphsphonothiolates [7], the reduced Sp/Rp ratio of EMP-4PAM can be attributed to a partial accommodation of the relatively small ethoxy group of the less potent stereoisomer in the acyl pocket of AChE.

The bimolecular rate constants for the inhibition of rMoAChE, FBS AChE, HuBChE, and EqBChE are summarized in Table 1. For rMoAChE and FBS AChE, all AlkMeP-2PAMs were 7- to 100-fold more potent than the parent OPs [22–24]. For example, replacement of F or $SCH_2CH_2N(iPr)_2$ in sarin and VX with 2-PAM, increased the k_i for rMoAChE from 0.014 and $0.12 \times 10^9\ M^{-1}\ min^{-1}$ to $1.42 \times 10^9\ M^{-1}\ min^{-1}$ (IMP-2PAM) and $1.94 \times 10^9\ M^{-1}\ min^{-1}$ (EMP-2PAM), respectively. Introducing 4-PAM as the leaving group also resulted in an increase in k_i relative to the parent compounds, however, to a lesser extent. AlkMeP-3PAMs were the least potent inhibitors of AChEs. In fact, the k_i values of EMP-3PAM and CMP-3PAM were reduced 3- to 5-fold relative to those of VX and cyclosarin, respectively.

Notably, increasing the size of the *O*-alkyl substituent of AlkMeP-POXs has only a small effect on the k_i for either enzyme, with the exception of the *O*-cyclohexyl ring. Of all the POXs tested, the maximal rate of inhibition was noted for CMP-2PAM ($4.02 \times 10^9\ M^{-1}\ min^{-1}$). Regardless of the oxime moiety, within a given POX series, the rigid cyclohexyl ring was associated with an increase in k_i for the inhibition of ChEs. An analogous increase in k_i was observed in a series of *O*-alkyl methylphosphonofluoridates such as sarin, soman, and cyclosarin [22,24]. Introducing a methyl group on the cyclohexyl ring (MCMP-POXs) resulted in a slight to moderate decrease in k_i that is attributable to steric constraints. The small but significant differences in k_i values for rMoAChE and FBS AChE, point to subtle structural differences in the catalytic gorge of these two enzymes.

Inhibition ranking order of POXs for BChEs differed significantly from that observed with AChEs. For example, all three DEP-POXs were found to be more potent inhibitors of HuBChE compared to AChEs, suggesting a better accommodation of DEP-POXs in the enlarged gorge [25]. The significantly slower rate of inhibition of EqBChE by POXs compared to HuBChE can be attributed to structural variations between the two BChEs.

Replacement of one of the ethoxy groups in DEP-POXs with the bulkier dimethylamino residue provides the expected tabun-type derivatives, EDMP-2PAM and EDMP-4PAM. These compounds are poor inhibitors of both AChEs and BChEs, an observation that is attributed to a combination of steric factors and a reduction in the electro-positivity of the phosphorus atom. Interestingly, the k_i of EDMP-2PAM was 3-fold lower for HuBChE compared to AChE.

Table 2
Semi-empirical calculations on POXs

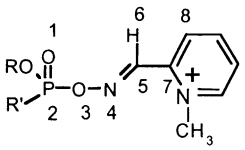

2-POX

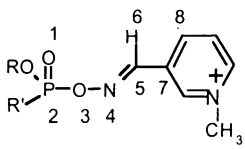

3-POX

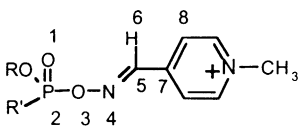

4-POX

POX	R	R′	Molecular electrostatic potentials (kcal/mol)			Dihedral angle (°)		
			O(1)	P(2)	H(6)	4–5–7–8	1–2–3–4	1–2–O–R
2-POXs								
EMP-2PAM	C_2H_5	CH_3	−55.5	142.3	94.2	133	40	29
IMP-2PAM	$CH(CH_3)_2$	CH_3	−57.0	145.0	96.5	−135	−41	1.7
PMP-2PAM	$CH(CH_3)C(CH_3)_3$	CH_3	−58.2	134.9	88.9	134	40	20
CMP-2PAM	Cyclohexyl	CH_3	−59.7	140.0	92.0	−132	−43	−4.5
MCMP-2PAM	2-Methylcyclohexyl	CH_3	−58.1	135.2	89.3	−146	−44	−22
DEP-2PAM	C_2H_5	C_2H_5	−59.6	146.9	96.6	−132	59	20
3-POXs								
EMP-3PAM	C_2H_5	CH_3	−65.3	137.8	89.2	−155	−39	3.9
CMP-3PAM	Cyclohexyl	CH_3	−65.7	134.0	86.5	−157	−39	2.2
DEP-3PAM	C_2H_5	C_2H_5	−60.7	128.8	82.7	−161	−49	−37
4-POXs								
EMP-4PAM	C_2H_5	CH_3	−68.0	132.7	84.3	166	41	30
IMP-4PAM	$CH(CH_3)_2$	CH_3	−68.3	133.4	85.0	167	41	19
PMP-4PAM	$CH(CH_3)C(CH_3)_3$	CH_3	−68.3	128.5	82.4	177	−43	−26
CMP-4PAM	Cyclohexyl	CH_3	−68.4	134.9	86.7	167	39	21
MCMP-4PAM	2-Methylcyclohexyl	CH_3	−67.8	132.1	84.3	166	37	22
DEP-4PAM	C_2H_5	C_2H_5	−63.8	131.8	84.9	171	53	39

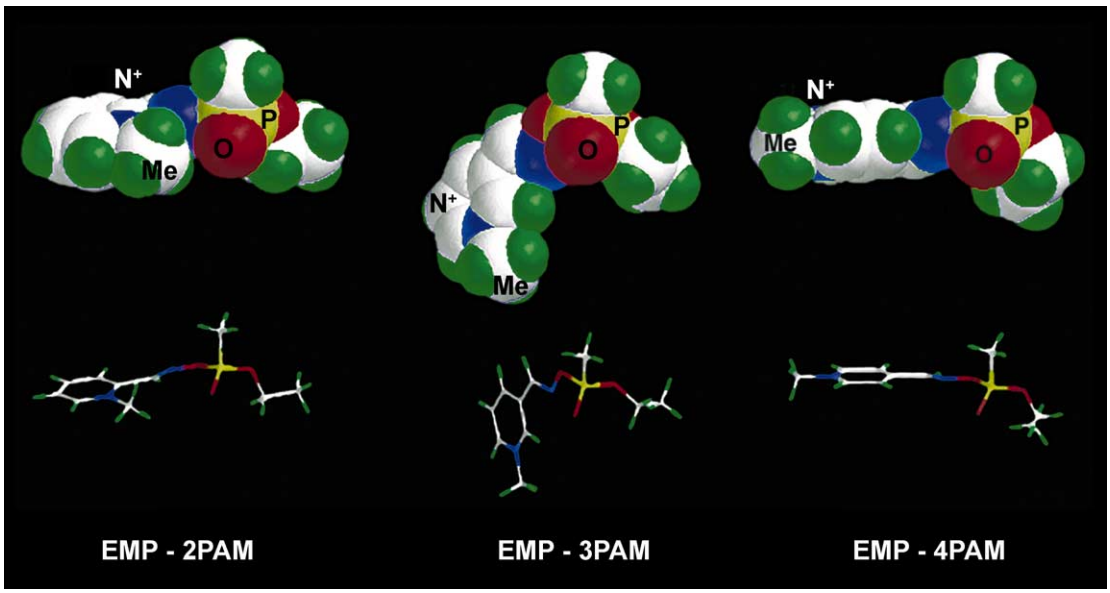

Fig. 3. Space-filled models for the 6-31G** optimized geometries of EMP-POXs. Color codes: Yellow, phosphorus; Red, oxygen; Blue, nitrogen; White, carbon; Green, hydrogen.

3.4. Molecular electrostatic features and low energy conformers

To substantiate some of the experimental conclusions, the electronic and geometric features of POXs were calculated using AM1 and *ab initio* quantum chemical methods using the 6-31G** basis set. The optimized geometry of IMP-4PAM was highly similar to its reported X-ray crystal structure [20]. For example, in the crystal structure, the O−N=C(H)−Cpyr plane was reported to be 14.2° to the best plane through the pyridine ring, an angle that is close to the calculated value of 13° (180° − 167°) for the N(4)−C(5)−C(7)−C(8) dihedral angle (Table 2). Further, the acidity rank order of 2-, 3-, and 4-PAM (pK_a 8.0, 9.2, and 8.6, respectively; [26]) correlated well with the rank order of the positive potential values of the acidic hydrogen of the hydroximino function of 2-, 3-, and 4-PAM (103.5, 96.5, and 98.2 kcal/mol, respectively). These values are a measure of the intrinsic acidity estimated by scanning the MEP surfaces. Thus, the existing experimental data validate the steric and electronic properties derived from these calculations.

The MEP values of O(1), P(2) and H(6) atoms for the three POX series are summarized in Table 2. The most positive electrostatic potential was found to be on the phosphorus atom and the most negative potential was associated with the P=O oxygen O(1). The 2-POX series displayed the greatest positive potential of the 6(H) atom, and thus, the strongest acidity. The acidity of the 6(H) atom in 3- and 4-POXs was similar. The AM1 and the *ab initio* calculations gave similar results. This discrepancy, can be reconciled by taking into account the possible steric hindrance that can affect the interaction between the positive charge of the pyridine ring and the P=O oxygen atom as illustrated for EMP-POXs in Fig. 3.

The low-energy-high-abundance conformers of the 2- and 4-POXs reveal some differences in the structure of the optimized geometry (Fig. 4, 2-POXs). CMP-, and MCMP-2PAM displayed similar O(1)−P(2)−O(3)−N(4) (−43 and −44°) dihedral angles, however, they differ more in the N(4)−C(5)−C(7)−C(8) (−132 and −146°) and O(1)−2(P)−O−R (−4.5 to −22°) dihedral angles. Yet, the k_i values of CMP-2PAM and MCMP-2PAM were about the same. On the other hand, despite differences in the optimized structures of EMP-2PAM, IMP-2PAM, and PMP-2-PAM, the k_i values were similar. This lack of correlation of the anti-ChE potency with a specific geometry was further pronounced with the 4-POX series.

4. Discussion

4.1. Decomposition of POXs

The salient characteristic of the stability study is the correlation between the calculated relative acidity of the 6(H) atom, P−O−N=C(H)−Cpyr of 2- and 4-POXs, and k_d. Thus, the more acidic the hydrogen, the less stable the POX. The acidity is influenced by through-space repulsion forces, which depend on the distance between the 6(H) atom and the positive charge of the pyridine ring. The optimized geometries shown in Fig. 3 indicate that the *N*-methyl group in EMP-2PAM interferes with any possible through-space interaction between the positive charge on the pyridine nitrogen and the most negative potential of the P=O oxygen. This enables the molecule to dissipate more of its positive charge and makes the 6(H) atom more acidic than in the other two POXs. In addition, resonance stabilization of the charge is expected to increase the acidity of

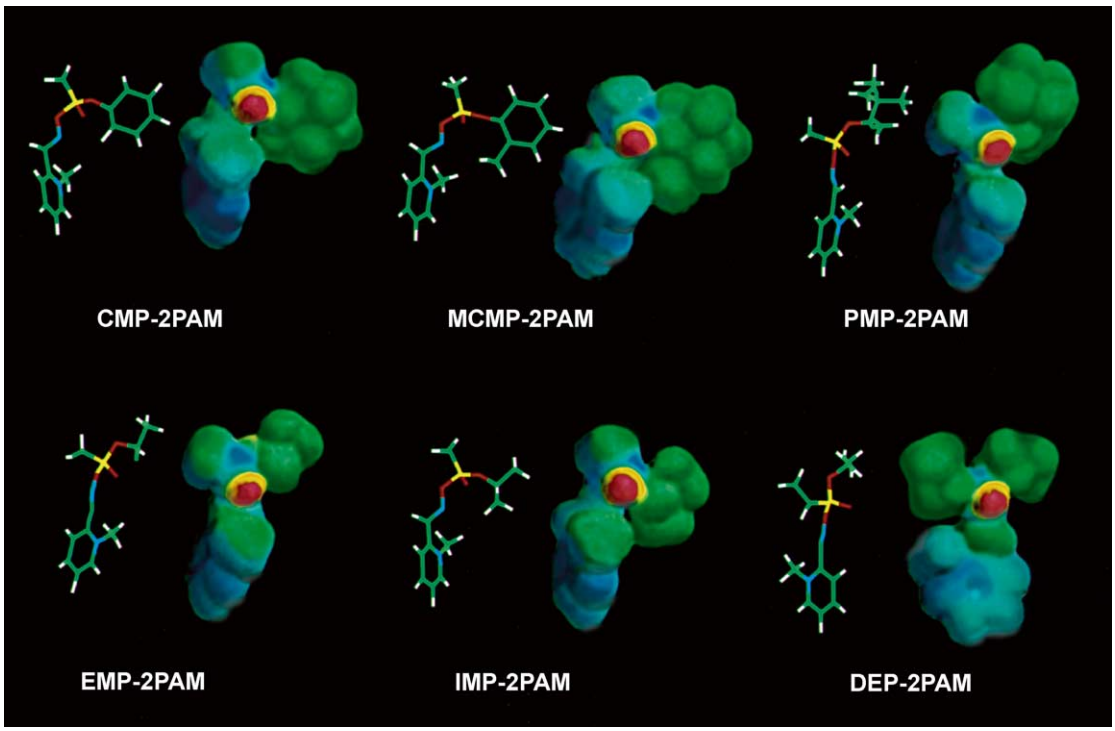

Fig. 4. Molecular electrostatic potential maps of the 6-31G** optimized geometries. Colors show the most positive potential (deepest blue) and the most negative potential (deepest red) regions of the 2-POX series.

6(H) in 2- and 4-POXs, while no such mechanism is possible in the 3-POXs (Fig. 2c). The average acidity of 6(H) in 2- and 4-POX series could be well correlated with their rate of decomposition, namely, the higher the acidity the less stable the POX. However, the 3-POXs that were similar in acidity to that of the 4-POXs were found to be at least 5-fold more stable than the 4-POXs. This discrepancy can be explained by the observation that the greatest interaction between the charged nitrogen and the negative potential on the P=O oxygen atom occurs in the least hindered EMP-3PAM (Fig. 3). This interaction is expected to decrease the attraction forces between the charged nitrogen and the base acceptor, which may slow down proton abstraction (Fig. 2b) and make the 3-POX series the most stable.

In each series, the decreased stability of DEP-POXs compared to the AlkMeP-POXs and EDMP-POXs, can be attributed to the pK_a of R′P(O)(OR)OH (Fig. 2b). Thus, *O*,*O*-diethylphosphoric acid ($R' = OC_2H_5$; $R = C_2H_5$; p$K_a = 1.04$) has a 10-fold higher acidity than the corresponding *O*-alkyl methylphosphonic acids ($R' = CH_3$; R = alkyl) [27]. It appears that the greater resonance stabilization of the negative charge on the conjugate base $(C_2H_5O)_2P(O)O^-$ compared to $CH_3P(O)(OR)O^-$, is responsible for the increased acidity, and is likely to accelerate decomposition of DEP-POXs. Also, replacement of CH_3-P with $(CH_3)_2N-P$ is not expected to change the poor pπ–dπ overlap between phosphorus and these substituents [28], and therefore, the acidities of $CH_3P(O)(OC_2H_5)OH$, and $(CH_3)_2NP(O)(OC_2H_5)OH$ are likely to be similar. Direct pK_a measurements, however, will be required to validate this suggestion.

In summary, it is likely that AlkMeP-POXs decompose via β-elimination reactions with rates that are strongly influenced by the structure of the PAM moiety and less by the nature of the *O*-alkyl susbstituent.

4.2. Inhibition of ChEs with POXs

Once the POXs are transferred from the aqueous solution to ChEs, the reaction center shifts from the 6(H) atom to the phosphorus atom and produces a substantial increase in the $S_N2(P)$ reaction. This is supported by the facts that DEP–ChE conjugates were obtained [15], and the k_i values for the inhibition of the four ChEs by AlkMeP-POXs and DEP-POXs increased with increasing acidity of the leaving groups.[4]

With the exception of the cyclohexyl derivatives, increasing the size of the *O*-alkyl substituent in AlkMeP-POXs had in general a small effect on the k_i for ChEs. These results differ from those reported for cationic aliphatic OPs [7], where 20- to 50-fold increases in k_i values for AChE and BChE were reported, respectively, when the *O*-isopropyl group was replaced with the *O*-3,3-dimethylbutyl group. The diminished dependency of k_i on the size of the *O*-alkyl substituent suggests that the

[4] pK_a values (2-PAM, 8.0; 4-PAM, 8.6; 3-PAM, 9.2) were reported by Ginsburg and Wilson [26] for a series of biologically reactive isomers that were later assigned the *syn* configuration ([29,30]; Fig. 1).

increased reactivity of POXs is mainly due to the interaction between the pyridinium ring and conserved residues such as D74 and W86 in AChE (D70 and W82 in HuBChE) [31]. Thus, it can be generalized that the cationic aromatic moieties that serve as leaving groups, contribute sufficient stabilization energy for the productive alignment of the inhibitor in the catalytic gorge.

Remarkable differences in the reactivity of AlkMeP-POXs and DEP-POXs were observed between AChEs and BChEs. Up to a 6-fold increase in the k_i value for the inhibition of rMoAChE compared to HuBChE was recorded with AlkMeP-2PAMs. However, the k_i values of AlkMeP-4PAM vary only slightly between the two enzymes, while EMP-3PAM and CMP-3PAM inhibited HuBChE 2- and 12-fold faster than rMoAChE. It seems that the location of the charged nitrogen in the pyridine ring determines the relative potency of POXs due to the different projections of the leaving groups in the gorge. One may argue that for the 2-PAM series, the enlargement of the acyl pocket, and near-by sites in HuBChE permits several low-level POX-enzyme adducts that eventually will slow down inhibition because of non-productive binding. Removing the hydroximinomethyl function away from the charged nitrogen apparently favors an orientation that increases the probability of expulsion of the leaving group in HuBChE and consequently the rate of inhibition. The latter is maximized with the AlkMeP-3PAMs, a finding that is consistent with the pyridinium oxime moiety being in a different orientation in its optimized structure compared to AlkMeP-2PAMs and AlkMeP-4PAMs (Fig. 3).

While AlkMeP-2PAMs were more potent inhibitors of AChEs compared to BChEs, all DEP-POXs-inhibited HuBChE 10- to 412-fold faster than the two AChEs. The fact that k_i values of cationic aliphatic OPs such as the DEP-containing inhibitors echothiophate, IMP-thiocholine, and its *O*-3,3-dimethylbutyl homologue [7] were similar for rMoAChE and HuBChE highlight the unique contribution of the cationic aromatic moiety to the enhanced inhibition of ChEs. The increase in inhibition potency of DEP-POXs toward HuBChE seems to be controlled by two factors: (1) the enlargement of the acyl pocket and choline binding site in HuBChE can accommodate DEPs and other bulky *O*-alkyl substituents [7,32,33] more comfortably than AChE; and (2) the enlarged gorge seems to provide more favorable interactions for charged aromatic DEPs (e.g. DEPQ, DEP-2, 3-, and 4-PAM), with functionally conserved residues such as D70 and W82 in HuBChE.

4.3. Analysis of linear-free energy relationships

The analysis of linear-free energy relationships was applied as a diagnostic tool for the further interpretation of the results of the inhibition studies.

4.3.1. Anti-ChE activity of cyclohexyl-containing OPs

The relationship between log k_i and the acidity of 2-, 3-, and 4-PAM was used to underscore the increased rate of inhibition by cyclohexyl-containing AlkMeP-POXs (Fig. 5). Despite the limited number of data points (N = 3 for each ChE) the use of Brönsted plots for the qualitative comparison of CMP-POXs with EMP- and DEP-POXs is valid because essentially similar shapes were obtained for all four ChEs. The lines in Fig. 5 clearly show that of all the POXs examined, the most potent CMP-POX series displayed the smallest dependency on the acidity of the leaving group. The decreased dependency of log k_i on pK_a can be considered as an indication of a change in the

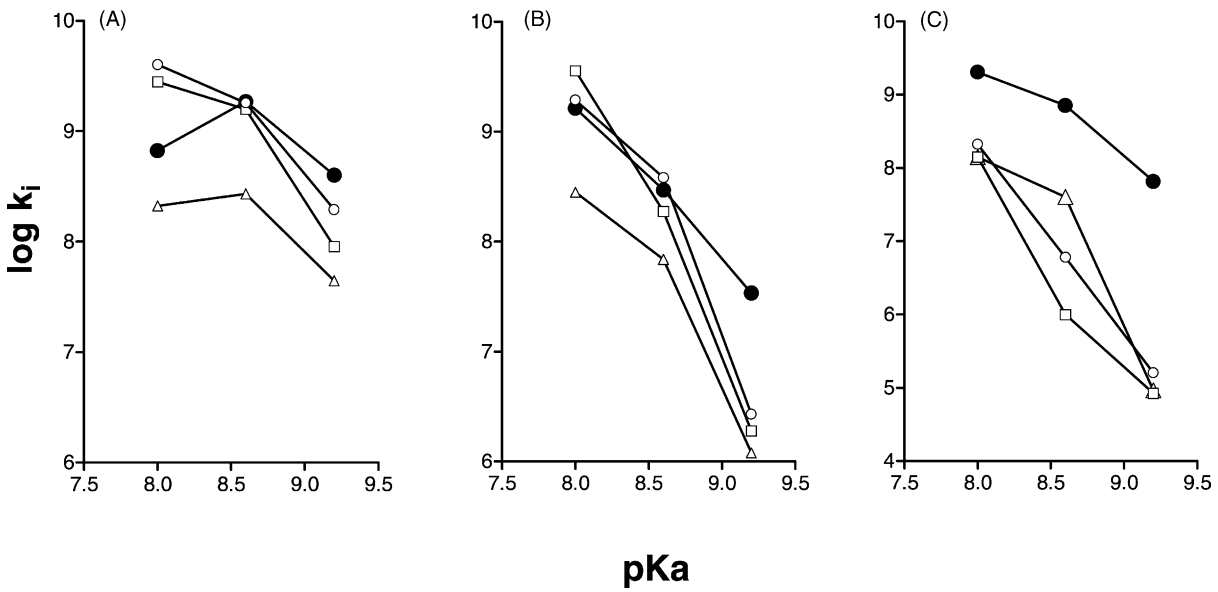

Fig. 5. Brönsted plots (log $k_i = \beta pK_a + C$) for the inhibition of ChEs by POXs. Panel A, CMP-POX; panel B, EMP-POX; and panel C, DEP-POXs (the leaving groups for each panel are 2-, 3-, and 4-PAM; pK_a taken from [26]. Symbols represent HuBChE (●), FBS AChE (□), EqBChE (△), and rMoAChE (○).

rate-determining step. A possible kinetic scheme that could account for the visual change in the Brönsted slopes is shown in Eq. (4). It involves the rapid formation of a reversible enzyme-POX complex (K_I) that follows a slow conformational change (k_c) prior to the unimolecular phosphonylation step (k_p). That OPs can induce considerable reversible conformational changes in AChE has been recently confirmed by X-ray crystallography [1,2]:

$$\mathrm{EOH} + \mathrm{POX} \overset{K_I}{\rightleftarrows} \mathrm{E{-}OH \cdot POX} \underset{k_{-c}}{\overset{k_c}{\rightleftarrows}} \mathrm{E{-}OH^{*}POX} \overset{k_p}{\rightarrow} \mathrm{E{-}O{-}P} + \mathrm{HX} \quad (4)$$

The second order rate constants for the inhibition of enzyme (EOH) activity were approximated as follows [34]:

$$k_p > k_{-c}, \quad k_i = \frac{k_c}{K_I} \quad (5)$$

$$k_p < k_{-c}, \quad k_i = \frac{k_c k_p}{K_I k_{-c}} \quad (6)$$

We assume that constants that reflect binding of POXs to AChE (i.e. K_I, k_c, k_{-c}) are relatively independent of the pK_a of the leaving group, while k_p must be highly dependent on it. The dependency of k_i on k_p will only be evident when $k_p < k_{-c}$ (Eq. (6)) which is probably the case with EMP-, and DEP-POXs. For the CMP-POX series it appears that $k_p > k_{-c}$, and therefore, k_i is significantly less dependent on the acidity of the leaving group (Eq. (5)). The greater activity of CMP-POXs is attributed to the cyclohexyl ring that is part of a pharmacophore that offers simultaneous multiple hydrophobic interactions with residues that are involved in the accommodation of OP ligands in the active-site gorge. The prevalence of $k_p > k_{-c}$ for CMP-POXs is reasonably explained on the basis of the tight binding to AChE that slows down k_{-c}. Of particular interest is the 72-fold increase in k_i of CMP-3PAM against rMoAChE relative to EMP-3PAM. Here, the contribution of the cyclic ring is greatly pronounced and appears to suppress unfavorable factors such as the reduced acidity of the leaving group, 3-PAM.

4.3.2. Reactivity of cationic aromatic vs. charged aliphatic OPs

Sharp curvatures in the plots of log k_i of enzymatic reactions vs. the pK_a of structurally unrelated leaving groups previously were observed around pK_a values of 7–8, for the inhibition of AChE by non-charged DEPs [4,34]. The hydroxide-catalyzed hydrolysis of DEPs including DEPQ,[5] and of other series of OPs, displayed linear log k_{OH} vs. pK_a plots over a wide range of pK_a values of leaving groups [34]. Therefore, the curvature observed with rMoAChE is peculiar to the enzymatic inhibition reaction. The nucleophilic attack by AChE at the phosphorous atom of DEP-MHP and DEP-3PAM (and probably

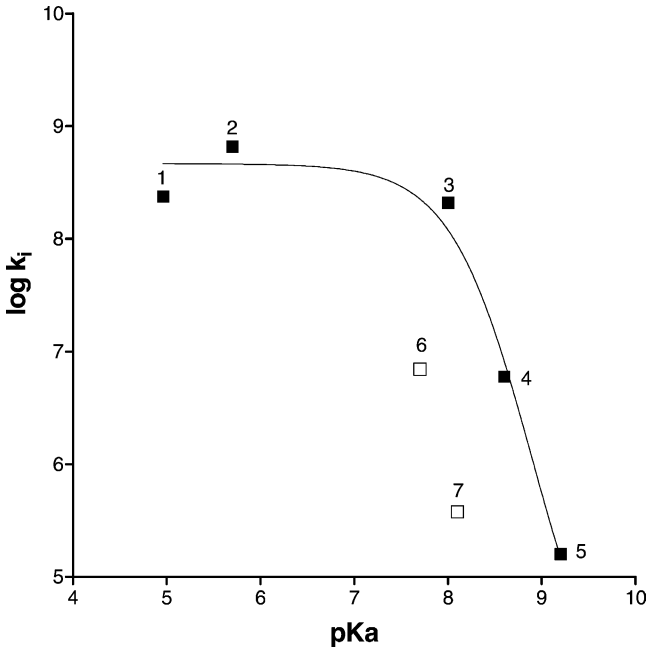

Fig. 6. Brönsted plot for the inhibition of rMoAChE by *O*,*O*-diethylphosphates. The numbers refer to the following DEPs: 1, DEP-MHP; 2, DEPQ; 3, DEP-2PAM; 4, DEP-4PAM; 5, DEP-3PAM; 6, echothiophate; 7, DEP-TMP. Symbols represent cationic aromatic DEPs (■) and charged aliphatic DEPs (□). For structural details see Fig. 1.

DEP-2 and DEP-4PAM), is not likely to differ sterically, and yet, the k_i values of DEP-MHP (pK_a 4.96; [35]) and DEPQ (that contains a different leaving group) leveled off in the Brönsted plot (Fig. 6). This break in the curve is indicative of a change in the rate-limiting step, the mechanism of which is most likely similar to that proposed for the scheme in Eq. (4). A sharp break at ~pK_a 8.0 recently was reported for phosphatase-induced hydrolysis of phenyl-containing substrates with relatively small structural alterations in the leaving group [36]. These observations, together with a slope >1 for the descending portion of the line, seem to indicate that bond breaking is advanced in the transition state [37,38]. It is possible that within a certain pK_a range, presumably below 8, the electron withdrawal capacity of the leaving group is an important driving force for the inhibition reaction by DEP-POXs.

Fig. 6 also shows that the k_i values of echothiophate and DEP-TMP for rMoAChE are 45- and 520-fold smaller, respectively, than would be predicted from their pK_a values. It is proposed that the greater anti-ChE activity of cationic aromatic DEPs is due to a combination of increased acidity of the leaving group and better complimentarity with the catalytic gorge that arises from the coupling of a positive charge to an aromatic system. The continuity of positive electrostatic potential on a planar pyridine ring with a large surface area is expected to provide more efficient contact with the π face of several aromatic planes in the gorge [39–46]. The importance of cationic aromatic systems in methylphosphonates is also evident from the fact that the k_i values of IMP-2PAM and

[5] Present study, data not shown.

IMP-4PAM are at least 89- and 7-fold greater than those reported for the inhibition of rMoAChE by the aliphatic inhibitor IMP-thiocholine.[6] This rationalization for the increased activity of charged aromatic DEPs appears to also hold for AlkMeP-POXs and MEPQ.

5. Conclusion

The experimental and theoretical study of POXs reveals distinct types of OP inhibitors of ChEs, and underscores the unique contribution of the charged pyridine moiety and the cyclohexyl group to the inhibition of ChEs. The orientation of the large aromatic cation that serves as the leaving group seems to be a result of tight interactions with conserved residues in AChE and BChE that also accelerate the inhibition reaction. A second generalization is that oxime-induced reactivation of AChE inhibited with *O*,*O*-diethyl-based phosphates (e.g. commercial pesticides), should be less complicated than that inhibited with nerve-agents. This is due to the rapid decomposition of DEP-POXs compared to AlkMeP-POXs and EDMP-POXs.

Finally, it was reported that soman- and cyclosarin-inhibited AChEs were reactivated more readily with 2-PAM derived oxime antidotes (HI-6, HS-6 and HLÖ7) than with the 4-PAM-based analogs (TMB4 and obidoxime) [24,47]. Results of this study suggest that this could be due in part, to the formation of stable and potent PMP- and CMP-4PAM based POXs with k_i values for ChEs that are likely to exceed 1×10^{10} M^{-1} min^{-1} [3]. Thus, the properties of POXs should be taken into consideration in the evaluation of kinetic studies on the reactivation and aging of OP-ChE conjugates.

Acknowledgments

The authors wish to thank SGT Connie Hinrichs for the excellent technical assistance.

References

[1] Millard CB, Koellner G, Ordentlich A, Shafferman A, Silman I, Sussman JL. Reaction products of acetylcholinesterase and VX reveal a mobile histidine in the catalytic triad. J Am Chem Soc 1999;121:9883–4.

[2] Millard CB, Kryger G, Ordentlich A, Greenblat HM, Harel M, Raves ML, Segall Y, Barak D, Shafferman A, Silman I, Sussman JL. Crystal structures of aged phosphonylated acetylcholinesterase: nerve agent reaction products at the atomic level. Biochemistry 1999;38:7032–9.

[3] Luo C, Saxena A, Smith M, Garcia G, Radic Z, Taylor P, Doctor BP. Phosphoryl oxime inhibition of acetylcholinesterase during oxime reactivation is prevented by edrophonium. Biochemistry 1999;38:9937–47.

[6] Values are for the Sp enantiomer of IMP-thiocholine [7], and should be divided by 2 to normalize the k_i to that of the racemic mixtures used in this work.

[4] Kitz RJ, Ginsburg S, Wilson IB. The reaction of acetylcholinesterase with diethylphosphoryl esters of quaternary and tertiary aminophenols. Mol Pharmacol 1967;3:225–32.

[5] Levy D, Ashani Y. Synthesis and in vitro properties of a powerful quaternary methylphosphonate inhibitor of acetylcholinesterase. A new marker in blood–brain barrier research. Biochem Pharmacol 1986;35:1079–85.

[6] Maglothin JA, Wilson IB. Equilibrium constants for the phosphorylation of acetylcholinesterase by some diethyl phosphorothiolates and phosphates. Biochemistry 1974;13:3520–7.

[7] Hosea NA, Berman HA, Taylor PM. Specificity and orientation of trigonal carboxyl esters and tetrahedral alkylphosphonyl esters in cholinesterases. Biochemistry 1995;34:11528–36.

[8] Radic Z, Quinn DM, Vellom DC, Camp S, Taylor P. Allosteric control of acetylcholinesterase catalysis by fasciculin. J Biol Chem 1995;270:20391–9.

[9] Heilbronn E. Hydrolysis of carboxylic acid esters of thiocholine and its analogues. 2. alkaline hydrolysis. Acta Chem Scand 1958;12:1492–506.

[10] Hackley BE, Owens OO. Preparation of *O*-(isopropylmethylphosphono)-4-formyl-1-methylpyridinium iodide oxime. J Org Chem 1959;21:1120.

[11] De Jong LPA, Ceulen DI. Anticholinesterase activity and rate of decomposition of some phosphylated oximes. Biochem Pharmacol 1978;27:857–63.

[12] Harvey B, Scott RP, Sellers DJ, Watts P. In vitro studies on the reactivation by oximes of phosphylated acetylcholinesterase-II. On the formation of *O*,*O*-diethyl phosphorylated AChE and *O*-ethyl methylphosphonylated AChE and their reactivation by PS2. Biochem Pharmacol 1986;35:745–51.

[13] Lamb JC, Steinberg GM, Solomon S, Hackley BE. Isopropyl methylphosphonylated bisquaternary oximes; powerful inhibitors of cholinesterases. Biochim Biophys Acta 1964;89:174–6.

[14] Nenner M. Phosphonylated aldoximes. Antagonism of acetylcholinesterase and hydrolytic decomposition. Biochem Pharmacol 1974;23:1255–62.

[15] Leader H, Vincze A, Manisterski B, Rothchild N, Dosoretz C, Ashani Y. Characterization of *O*,*O*-diethylphosphoryl oximes as inhibitors of cholinesterases and substrates of phosphotriesterases. Biochem Pharmacol 1999;58:503–15.

[16] Gordon MA, Carpenter DE, Barret HW, Wilson IB. Determination of the normality of cholinesterase solutions. Anal Biochem 1978;85:519–27.

[17] De La Hoz D, Doctor BP, Ralston JC, Rush RS, Wolfe AD. A simplified procedure for the purification of large quantities of fetal bovine serum acetylcholinesterase. Life Sci 1986;39:195–9.

[18] Grunwald J, Marcus D, Papier Y, Raveh L, Pittel Z, Ashani Y. Large-scale purification and long-term stability of human butyrylcholinesterase: a potential bioscavenger drug. J Biochem Biophys Methods 1997;34:123–35.

[19] Ellman GL, Courtney KD, Andres V, Featherstone RM. A new and rapid colorimetric determination of acetylcholinesterase activity. Biochem Pharmacol 1961;7:88–95.

[20] Portmann R, Neiederhauser A, Hofman W, Frey A. Synthesis of 4-({[isopropyloxy]methylphosphonyloxy}iminomethyl)-1-methylpyridinium iodide and its characterization. Helv Chim Acta 1991;74:331–5.

[21] Hall CR, Inch TD, Inns RH, Muir AW, Sellers DJ, Smith AP. Differences between some biological properties of enantiomers of alkyl *S*-alkyl methylphosphonothioates. J Pharm Pharmacol 1977;29:574–6.

[22] Gray PJ, Dawson RM. Kinetic constants for the inhibition of eel and rabbit brain acetylcholinesterase by some organophosphates and carbamates of military significance. Toxicol Appl Pharmacol 1987;91:140–4.

[23] Raveh L, Grunwald J, Marcus D, Papier Y, Cohen E, Ashani Y. Human butyrylcholinesterase as a general prophylactic antidote for nerve agent toxicity. In vitro and in vivo quantitative characterization. Biochem Pharmacol 1993;22:2465–74.

[24] Worek F, Eyer P, Szinicz L. Inhibition reactivation and aging kinetics of cyclohexylmethylphosphonofluoridate-inhibited human cholinesterases. Arch Toxicol 1998;72:580–7.
[25] Saxena A, Redman AMG, Jiang X, Lockridge O, Doctor BP. Differences in active-site gorge dimensions of cholinesterases revealed by binding of inhibitors to human butyrylcholinesterase. Biochemistry 1997;36:14642–51.
[26] Ginsburg S, Wilson IB. Oximes of the pyridine series. J Am Chem Soc 1957;79:481–5.
[27] Van Hooidonk C, Kraaij GW, Ginjaar L. On the reactivity of organophosphorus compounds. Part IV: The alkaline hydrolysis of some *O*-phosphylated 2-pyridine oximes. Rec Trav Chem 1968;87:673–86.
[28] Kirby AJ, Warren SG. The organic chemistry of phosphorus. Amsterdam, London, New York: Elsevier; 1967.
[29] Poziomek EJ, Kramer DN, Mosher WA, Michel HO. Configurational analysis of 4-formyl-1-methylpyridinium iodide oxime and its relationship to a molecular complementarity theory on the reactivation of inhibited acetylcholinesterase. J Am Chem Soc 1961;83:3916–7.
[30] Carlstrom D. A crystallographic study of *N*-methyl-pyridine-2-aldoxime (2-PAM) halides. Acta Chem Scand 1966;20:1240–6.
[31] Harel M, Sussman JL, Krecji E, Bon S, Chanal P, Massoulie J, Silman I. Conversion of acetylcholinesterase to butyrylcholinesterase: modeling and mutagenesis. Proc Natl Acad Sci USA 1992;89:10827–31.
[32] Vellom DC, Radic Z, Li Y, Pickering NA, Camp S, Taylor P. Amino acid residues controlling acetylcholinesterase and butyrylcholinesterase specificity. Biochemistry 1993;32:12–7.
[33] Ordentlich A, Barak D, Kromman C, Ariel N, Segall Y, Velan B, Shafferman A. The architecture of human acetylcholinesterase active center probed by interactions with selected organophosphate inhibitors. J Biol Chem 1996;271:11953–62.
[34] Ashani Y, Snyder SL, Wilson IB. Linear free energy relationships in the hydrolysis of some inhibitors of acetylcholinesterase. J Med Chem 1973;16:446–50.
[35] Albert A, Phillips JN. Ionization constants of heterocyclic substances. Part II. Hydroxy-derivatives of nitrogenous six-membered ring compounds. J Chem Soc [Perkin 1] 1956;Part II:1294–304.
[36] McCain DF, Cartina IE, Hengge AC, Zhang Z-Y. The catalytic mechanism of Cdc25A phosphatase. J Biol Chem 2002;277:11190–200.
[37] Kirby AJ, Varvoglis AG. The reactivity of phosphate esters. Monoester hydrolysis. J Am Chem Soc 1967;89:415–23.
[38] Andres GO, Granados AM, de Rossi RH. Kinetic study of the hydrolysis of phthalic anhydride and aryl hydrogen phthalates. J Chem Soc [Perkin 1] 2001;66:7653–7.
[39] Ma JC, Dougherty DA. The cation–π interaction. Chem Rev 1997;97:1303–24.
[40] Zoltewicz JA, Maier NM. π-Cation and π-dipole-stabilizing interactions in a simple model system with cofacial aromatic rings. J Org Chem 1998;63:4985–90.
[41] Sussman JL, Harel M, Frolow F, Oefner C, Goldman A, Toker L, Silman I. Atomic structure of acetylcholinesterase from *Torpedo californica*: a prototypic acetylcholine-binding protein. Science 1991;253:872–9.
[42] Harel M, Schalk I, Ehert-Sabatier L, Bout F, Goeldner M, Hirth C, Axelson PH, Silman I, Sussman JL. Quaternary ligand binding to aromatic residues in the active-site gorge of acetylcholinesterase. Proc Natl Acad Sci USA 1993;90:9031–5.
[43] Radic Z, Pickering NA, Vellom DC, Camp S, Taylor P. Three distinct domains in the cholinesterase molecule confer selectivity for acetyl- and butyrylcholinesterase inhibitors. Biochemistry 1993;32:12074–84.
[44] Ordentlich A, Barak D, Kronman C, Flashner Y, Leitner M, Segall Y, Ariel N, Cohen S, Velan B, Shafferman A. Dissection of the human acetylcholinesterase active center determinants of substrate specificity. Identification of residues constituting the anionic site, the hydrophobic site. and the acyl pocket. J Biol Chem 1993;268:17083–95.
[45] Quinn DM, Feaster SR, Nair HK, Baker NA, Radic Z, Taylor P. Delineation and decomposition of energies involved in quaternary ammonium binding in the active site of acetylcholinesterase. J Am Chem Soc 2000;122:2975–80.
[46] Hosea NA, Radic Z, Tsigelny I, Berman HA, Quinn DM, Taylor PM. Aspartate 74 as a primary determinant in acetylcholinesterase governing specificity to cationic organophosphonates. Biochemistry 1996;35:10995–1004.
[47] De Jong LPA, Wolring GZ. Stereospecific reactivation by some Hagedorn-oximes of acetylcholinesterases from various species including man, inhibited by soman. Biochem Pharmacol 1984;33:1119–25.